

An Improved Method to Calculate the Gas Pressure History from Partially Confined Detonations

Charles Oswald Ph.D, P.E.; Protection Engineering Consultants, San Antonio, TX, USA

Abstract

This paper discusses an improved fast-running method to calculate the gas pressure history from an internal detonation in an explosion room with venting. It's development is an intermediate step towards a final, well validated, gas pressure prediction model for DDESB that is significantly more accurate compared to test data than the current method. As a first step in this research project, gas pressure data from over 100 confined and partially confined blast tests were gathered and put into a gas pressures database. The existing FRANG and BlastX codes were then used to model each of the tests and the calculated peak gas pressures and impulses were compared to measured values. Also, an initial improved methodology, which combined parts of FRANG and BlastX, was compared to the test data. These comparisons showed that all three gas pressure prediction methods were generally very conservative compared to the test data. Based on trends noted in these comparisons, the current improved methodology was developed to include a calculated rise time history for the gas pressure and to consider the effects of mass loss, room volume change due to vent panel movement, and energy loss when venting occurs during the rise time. This improved version, which has been programmed into an Excel spreadsheet, compares much better to measured gas pressure data than the existing methods. It is currently under review by the DoD. DDESB is also sponsoring additional gas pressure testing to address a lack of gas pressure test data for explosion rooms with a low loading density and large covered vent areas. This test data will be used to develop the final version of the improved methodology.

Keywords: gas pressure, internal detonations, venting

Introduction

A large database of internal detonation tests have been performed to measure the quasistatic, or gas pressure, in the explosion room from an internal detonation, including many tests where the measured pressure history is published. These tests have been gathered into a electronic database for the DDESB (Oswald, 2017). Most of these tests were performed in the 1970s and 1980s by the U.S. Navy, and were used to develop the empirical equations for the FRANG computer code that is currently used by the DoD Explosive Safety Board (DDESB) to calculate the gas pressure in the explosion room for explosive safety designs. FRANG calculates the peak gas pressure in the explosion room and venting of the gas pressure through openings in the room to the atmosphere, including openings that are initially covered with a panel (Wager and Connett, 1989). For the case of a covered opening, the internal shock and gas pressure are assumed to cause the panel to move away from the opening as a rigid body with negligible attachments to the wall or roof of the explosion room. The calculated vent area at each time step is equal to the panel perimeter multiplied by the distance the panel has deflected away from the explosion room, up to the full area of the initially covered opening (Tancroto and Helseth, 1984). Modeling venting through vent areas that are originally covered by panels is a critical capability because many DoD operation bays have large, lightweight exterior walls and/or roofs that are intended to fail quickly in the event of an accidental internal detonation to allow venting as they are blown away from the bay.

Other agencies in the DoD use the BlastX computer code to calculate the shock and gas blast pressures in the explosion room, and surrounding rooms, from internal detonations. BlastX uses a thermochemical approach to calculate the peak gas pressure, which is based on the chemical reaction equation for the explosive and the heats of formation for the chemical products and reactants. It uses a first principles approach to calculate venting through uncovered vent areas by modeling this as an adiabatic process for isentropic flow of an ideal gas through a nozzle (Bessette and Emmanuelli, 2014). BlastX calculates venting through an opening that is initially covered by

unrealistically assuming the full area of the opening is available for venting immediately when an input failure condition for the panel is met, instead of modeling a gradual transition of the vent area from fully covered to fully open. This approach may change as part of major revision to BlastX that is ongoing.

The DDESB recently funded a project to gather and compare a database of measured gas pressure histories from internal detonation tests to gas pressures calculated for each test with FRANG 2.0, as incorporated into the CONBLAST (NAVFAC ESC, 2015) and BlastX V6.4.2.2 (ERDC). This study showed that the empirical method in FRANG and the thermochemical approach in BlastX calculate similar peak gas pressures for common high explosives in confined volumes that compare well to peak gas pressures measured in tests where the test room had minimal venting during the gas pressure rise time. However, the study showed that both FRANG and BlastX generally calculated much larger peak gas pressure and impulse (i.e. were over-conservative) compared to the gas pressures measured in tests where there was significant venting (Oswald, 2017).

This project also included work to develop an improved gas pressure methodology in a two-step approach. In the first step, an initial improved methodology was developed by combining the most accurate parts of the FRANG and BlastX into a simplified, fast-running methodology for DDESB. This consisted of combining the empirical approach in FRANG to calculate the peak gas pressure with a simplified version of the theoretical approach used in BlastX to calculate gas pressure venting. Also, the perimeter venting approach in FRANG for vent areas that are initially covered with a panel was included. This method overcalculated the peak gas pressure in the same manner as the FRANG code and generally calculated the gas pressure impulse better than both FRANG and BlastX for tests with venting in comparisons where all three calculation methods were modified to force a calculated peak gas pressure equal to the measured peak gas pressure. This correction was necessary so that accuracy of the venting models in these prediction methods could be compared to the test data without being affected by the fact all the methods significantly over-calculated the measured peak gas pressure.

Since the initial improved gas pressure methodology significantly overcalculated the peak gas pressure for tests with significant venting, the current improved gas pressure methodology was developed. This is the primary topic of this paper. The DDESB is currently funding additional one-half scale gas pressure tests to develop more test data that is representative for typical explosive operations bays with large wall and roof vent areas, which will be used to modify the current improved methodology as necessary to develop the final improved methodology.

Peak Gas Pressure in Improved Methodology

The current improved gas pressure methodology calculates a gas pressure history based on; 1) the peak gas pressure that would occur if the explosion room was fully confined, P'_g , 2) an assumed time history for the gas pressure rise to peak gas pressure in a fully confined volume, 3) the effects of room volume change, mass loss, and energy loss from the explosion room during the gas pressure rise time. The latter consideration reduces the peak gas pressure in cases where the explosion room has significant venting during the gas pressure rise time. Step 1 in this process calculates P'_g using the existing methodology in UFC 3-340-02 (2014). In the next step, P'_g is used to calculate the peak gas pressure that would occur with no afterburning, P'_{gd} , and the peak gas pressure due to afterburning, P'_{gab} , in a fully confined volume using Equation 1 and Equation 2. Equation 1 calculates W_{Ed} , which is used with the free volume of the explosion room in Figure 2-152 from UFC 3-340-02 to calculate the peak gas pressures caused by the detonation process, P'_{gd} . The peak gas pressures caused by afterburning, P'_{gab} , is calculated by subtraction with Equation 2. At charge weight to confined volume ratios (i.e. loading densities) greater than 0.1 lb/ft³, P'_{gab} is always equal to zero. There is not sufficient oxygen available in the confined volume for significant afterburning at these high loading densities (Proctor, 1972). Further testing and research may show that it is not necessary to separate the peak gas pressures caused by the detonation and by afterburning in the improved methodology.

$$W_{Ed} = \frac{H_{EXP}^d}{\phi [H_{TNT}^c - H_{TNT}^d] + H_{TNT}^d} W_{EXP}$$

Equation 1

where:

W_{Ed} = equivalent TNT charge weight for peak gas pressure without any afterburning
 H_{TNT}^c = heat of combustion of TNT
 ϕ = TNT conversion factor based on W/V ratio from Figure 2-166 in UFC 3-340-02
 H_{TNT}^d = heat of detonation of TNT
 H_{EXP}^d = heat of detonation of explosion in question
 W_{EXP} = weight of explosive of interest

$$P'_{g-ab} = P'_g - P'_{g-d}$$

Equation 2

where:

P'_g = peak gas pressure calculated using the method in UFC 3-340-02
 P'_{g-d} = peak gas pressure caused by the detonation process with no afterburning calculated using W_{Ed} and the free volume of the explosion room in Figure 2-152 from UFC 3-340-02
 P'_{g-ab} = peak gas pressure caused by the afterburning process

Gas Pressure Rise Time in Improved Methodology

An equation to calculate the gas pressure rise time to its peak pressure in a fully confined volume was developed by reviewing previous equations in the literature and modifying them as necessary to match the very limited available test data. This resulted in Equation 3 to calculate the gas pressure rise time, t_r . This equation is similar to that proposed by Hager et al. (2006), except with a different value for K_r . The rise time in this equation is equal to the time required for the shock wave to propagate across the explosion room 4.5 times (i.e. $K_r=4.5$), where the time required for the shock wave to propagate once across the room is equal to L_{max}/C_s . The logic for relating the gas pressure rise time to shock wave propagation time is that; 1) the shock wave disperses the detonation products and hot gases from the detonation throughout the volume, and 2) the shock wave dissipates into heat energy, as it propagates across the room volume (Hager et al. 2006).

$$t_r = K_r \frac{L_{max}}{C_s}$$

$$\text{where } C_s = \sqrt{\gamma(\gamma - 1)I_t} \quad \text{and} \quad I_t = \frac{(I_{amb} + I_{det} + I_{ab})}{(M_{air} + M_{exp})}$$

$$I_{det} = H_{det}W_{exp} \quad \text{and} \quad I_{ab} = \phi(H_{comb} - H_{det})W_{exp}$$

Equation 3

where:

t_r = maximum gas pressure rise time (i.e. in a fully confined volume)
 L_{max} = maximum dimension of the confined volume
 C_s = average shock velocity in confined volume
 I_{amb} = energy of air in volume at ambient conditions
 I_{det} = energy from conversion of shock energy to gas pressure
 I_{ab} = energy from combustion of detonation products
 I_{tot} = total energy density in volume after explosion
 H_{det} = heat of detonation for explosive
 H_{comb} = heat of combustion for explosive
 ϕ = TNT conversion factor based on W/V ratio from UFC 3-340-02
 W_{exp} = explosive charge weight
 M_{exp} = mass of explosive
 M_{air} = mass of air in explosion room
 K_r = empirical factor for rise time = 4.5

The gas pressure history during its rise time is calculated using Equation 4. This equation is based on a similar equation proposed by Hager et al. (2006), except that Equation 4 also includes a linear decay component. The linear

decay component causes the calculated gas pressure to rise all the way to the peak gas pressure, P'_g , at a time equal to t_r . The constants in Equation 4 are based on curve-fits to limited test data. Figure 1 shows a comparison of the gas pressure rise time history calculated by Hager et al (2006) and with Equation 4 using dimensionless parameters.

$$P_g(t) = P'_g \left[1 - e^{-\left(\frac{K_g t}{t_r}\right)} \left(1 - \frac{t}{t_r}\right) \right]$$

Equation 4

where:

- $P_g(t)$ = gas pressure during rise time in a fully confined volume (when $t \leq t_r$)
- P'_g = calculated peak gas pressure in a fully confined volume using method in UFC 3-340-02
- t_r = gas pressure rise time in a fully confined volume
- K_g = empirical factor for rise time history = 3.0
- t = time for $t \leq t_r$

Equation 3 and Equation 4 define a rise time history of the gas pressure in a fully confined volume. Equation 4 can be refined into two separate equations with the same form, as shown in Equation 5. The first equation for $P_{g,d}(t)$ calculates the gas pressure history during the rise time caused by the detonation. The second equation for $P_{g,ab}(t)$ calculates the gas pressure history from afterburning during its rise time. $P'_{g,d}$ and $P'_{g,ab}$ in Equation 5 are the peak gas pressures from the detonation and from afterburning, respectively, calculated with Equation 1 and Equation 2.

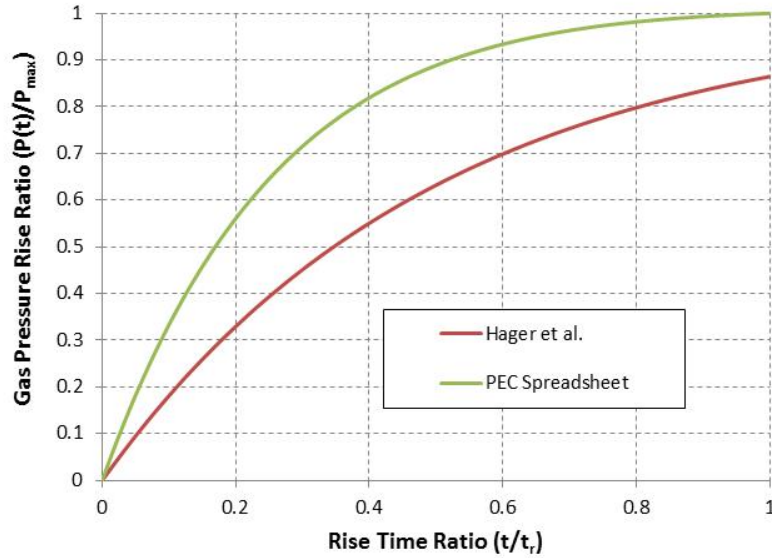


Figure 1. Non-Dimensionalized Rise Time from Improved Methodology and Hager et al.

$$P_{g,ab}(t) = P'_{g,ab} \left[1 - e^{-\left(\frac{K_g t}{t_r}\right)} \left(1 - \frac{t}{t_r}\right) \right]$$

$$P_{g,d}(t) = P'_{g,d} \left[1 - e^{-\left(\frac{K_g t}{t_{r,d}}\right)} \left(1 - \frac{t}{t_{r,d}}\right) \right]$$

Equation 5

where:

- $P_{g,d}(t)$ = gas pressure history during rise time caused by energy from detonation in a fully confined volume
- $P'_{g,d}$ = peak gas pressure caused by detonation in full confinement
- K_g = empirical factor for rise time history = 3.0
- $P_{g,ab}(t)$ = gas pressure history during rise time caused by afterburning in a fully confined volume

P'_{g_ab} = peak gas pressure caused by afterburning in full confinement
 t_r = gas pressure rise time from Equation 3
 t_{r_d} = rise time for gas pressure caused by detonation = $t_r/1.5$
 t = time for $t \leq t_r$

Figure 2 shows comparisons of the gas pressure history calculated during the rise time with $P_{g_d}(t)$ in Equation 5 and with Equation 4 to the measured gas pressure histories from tests where identical 1.93 lb. TNT charges were detonated with full confinement in nitrogen (no afterburning) and air (full afterburning) (Kuhl et al, 1998). The test data in Figure 2 shows measured pressures that are averaged over a moving 7.5 msec window, which minimizes the pressure fluctuations caused by the shock wave to better represent the gas pressure. The blue curve in Figure 2 was calculated using $P_{g_d}(t)$ from Equation 5 and the red curve was calculated using Equation 4. Figure 3 shows more comparisons of the gas pressure history calculated during the rise time with Equation 4 and measured pressure histories from fully confined tests with TNT in air (Keenan and Wager, 1992) (Weibull, 1968). Both tests had complete afterburning. In summary, the limited data in Figure 2 and Figure 3 indicate that Equation 4 and Equation 5 calculate the gas pressure rise with sufficient accuracy for a fast-running methodology.

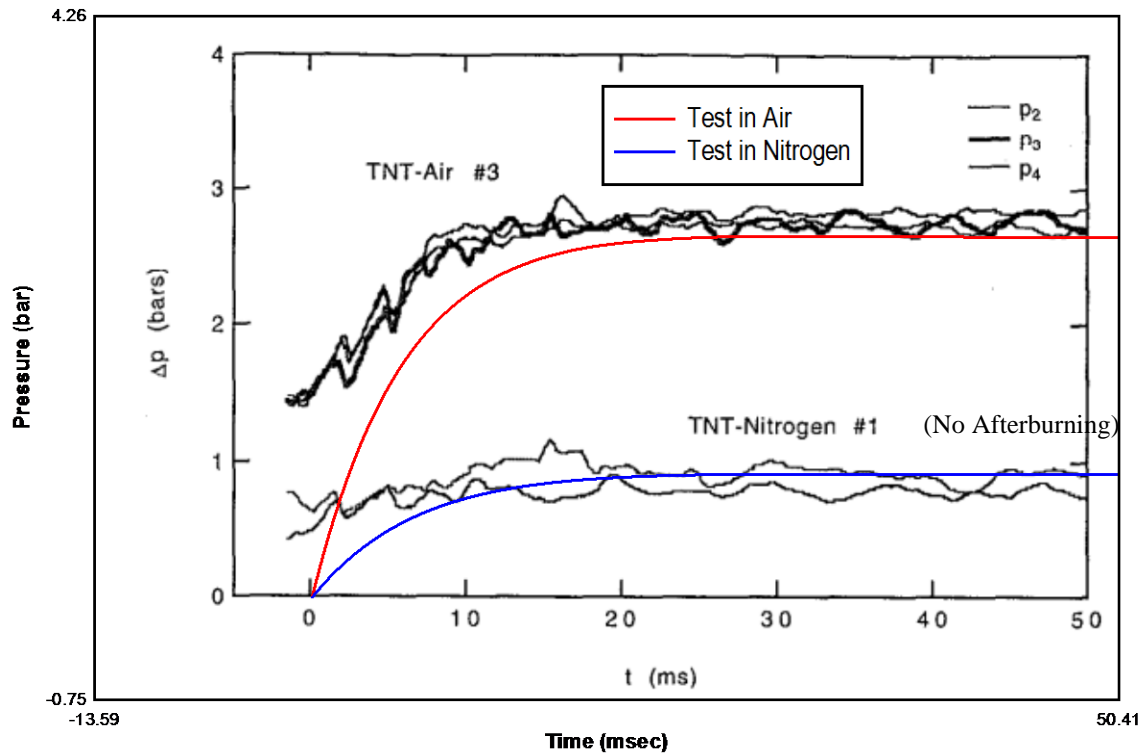
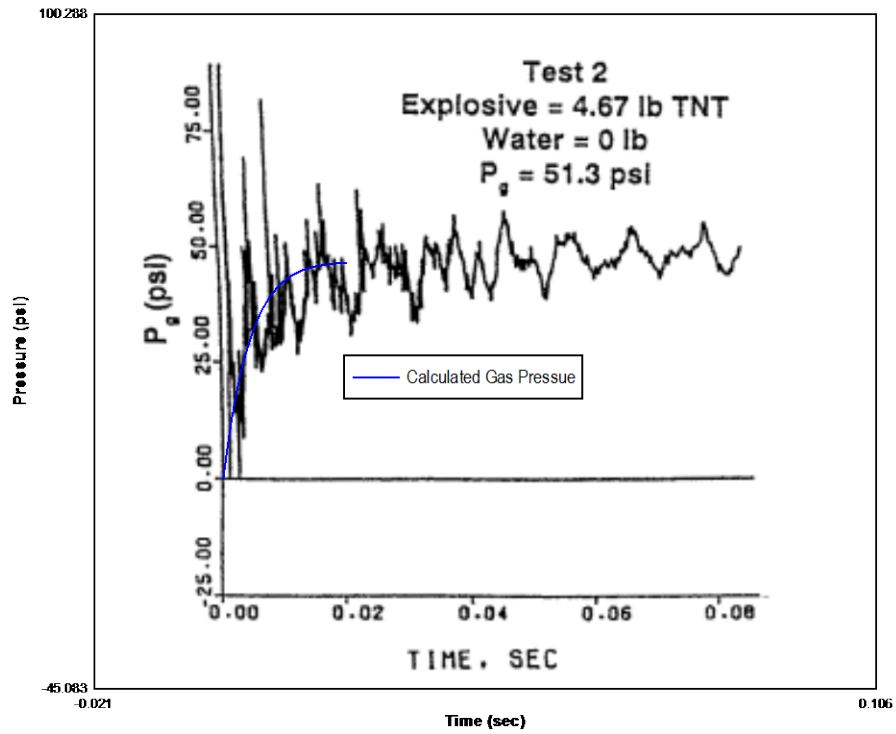


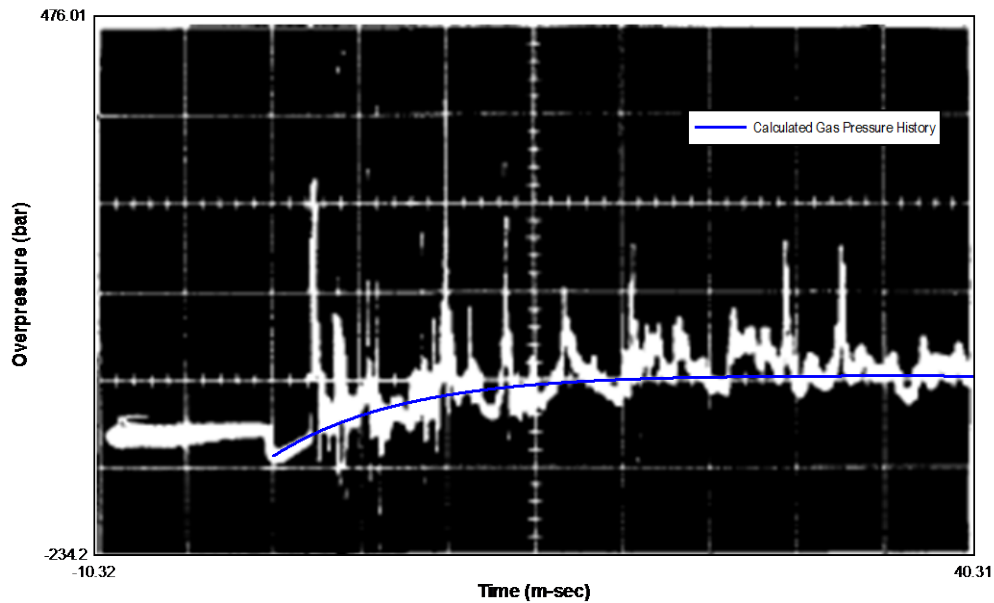
Figure 2. Comparisons of Calculated Gas Pressure Rise Histories with Fully Confined TNT Tests with Tests in Air and Nitrogen

Calculation of Gas Pressure History in Improved Methodology

The gas pressure is calculated at each time step during the rise time using Equation 6. Based on this equation, the gas pressure is equal to the pressure at the previous time step, modified by the factor $K_d(t)$ to account for any density change in the explosion room during the time step (i.e. room volume change and/or mass outflow through vent areas), plus any pressure rise during the time step. Pressure rise can only occur at time steps during the rise time, t_r . It is equal to the pressure rise calculated with Equation 5 caused by energy from the detonation and from afterburning, that is reduced by the empirical factor $K_{rf}(t)$ if there is any venting during the time step to account for energy loss through the vent area. The gas pressure rise (i.e. $\Delta P_{g_d}(t)$ and $\Delta P_{g_ab}(t)$) in Equation 6) is largest at early times and reduces at time steps near the end of the rise time, as shown in Figure 1.



a) NCEL test in confined explosion room (full afterburning)



b) Weibull test data (full afterburning)

Figure 3. Comparisons of Calculated Gas Pressure Rise Histories with Fully Confined TNT Tests (Full Afterburning)

$$\begin{aligned}
P_g(t) &= P_g(t-1)K_d(t) + [\Delta P_{g_d}(t) + \Delta P_{g_{afb}}(t)]K_{rf}(t) & \text{for } t \leq t_r \\
P_g(t) &= P_g(t-1)K_d(t) & \text{for } t > t_r
\end{aligned}$$

$$K_d(t) = \left(\frac{\rho(t)}{\rho(t-1)} \right)^\gamma = \left(\frac{M(t)}{V(t)} \right)^\gamma \left(\frac{V(t-1)}{M(t-1)} \right)^\gamma$$

Equation 6

- where: $P_g(t)$ = total gas pressure at time step t
 t_r = gas pressure rise time (see Equation 3)
 $\Delta P_{g_d}(t)$ = increase in the gas pressure caused by the detonation with no venting during time step (see Equation 5)
 $\Delta P_{g_{ab}}(t)$ = increase in gas pressure caused by afterburning with no venting during time step (see Equation 5)
 $K_d(t)$ = gas pressure reduction factor due to density change during time step based on Equation 8
 $\rho(t)$ = density of gas in explosion room at time t
 $M(t)$ = mass of gas in explosion room at time t (see Equation 9)
 $V(t)$ = effective volume of explosion room at time t (see Equation 14)
 γ = ratio of specific heats for air = 1.4
 $K_{rf}(t)$ = energy reduction factor accounting for energy loss due to venting during time step t (see Equation 7)

The density reduction factor $K_d(t)$ in Equation 6 is derived from the ideal gas law assuming adiabatic expansion of the room volume due to movement of covered vent area and mass loss from venting, as discussed later in this paper. The energy reduction factor $K_{rf}(t)$ in Equation 6 is calculated as shown in Equation 7. The equation for $K_{rf}(t)$ was developed empirically using curve-fitting and trial and error to minimize the difference between the maximum gas pressures calculated using trial equations for $K_{rf}(t)$ and measured values from the test data with uncovered vent areas. It was hypothesized based on initial efforts that $K_{rf}(t)$ was a function of the room gas pressure and trial forms of Equation 7 were used to calculate $K_{rf}(t)$ in Equation 6 until the peak gas pressures for all the applicable tests in the gas pressure database agreed well, on the average, with the measured maximum gas pressures. In later analyses for gas pressure tests with vent areas initially covered with a vent panel, Equation 7 was also found to cause a good match between calculated and measured gas pressure when the equations discussed later in this paper were used to calculate the time-varying vent area and room volume caused by movement of the vent panel during the gas pressure rise time. Note that $K_{rf}(t)$ does not influence the gas pressure at any time step greater than the gas pressure rise time, t_r , in Equation 6. The energy loss included in $K_{rf}(t)$ is assumed to be only energy that would otherwise contribute to the peak gas pressure. Also, $K_{rf}(t)$ is always 1.0 if the scaled vent area is less than 0.015 since existing methods to calculate peak gas pressure agree well with measured peak gas pressure in tests with scaled vent areas less than this very small value. The values of K_{rf} are higher for explosion rooms with a higher loading density since the high loading density causes larger values of $P_g(t)$ at each time step during the rise time.

$$K_{rf}(t) = \left(\frac{P_g(t-1)}{P_a} \right)^{K_p}$$

If: $\frac{A_v(t)}{V(t)^{\frac{2}{3}}} < 0.015$ then $K_p = 0$ Else: $K_p = -0.18$

Equation 7

- where: $K_{rf}(t)$ = gas pressure reduction factor to account for energy loss due to venting during time step
 $A_v(t)$ = vent area during time step calculated using Equation 11 and Equation 12
 $V(t)$ = explosion room volume during time step calculated using Equation 14
 $P_g(t-1)$ = total gas pressure at previous time step
 P_a = atmospheric pressure
 K_p = gas pressure reduction coefficient
Note: Vent area and volume are constant in explosion rooms with only uncovered vent areas

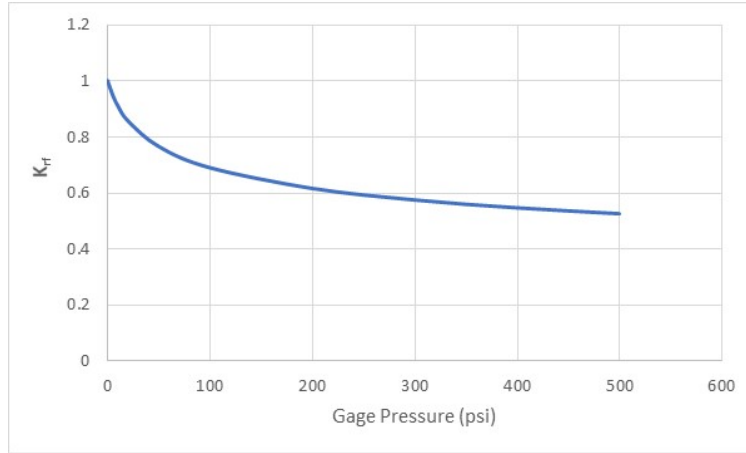


Figure 4. Reduction Factor for Energy Loss During Venting (K_{rf})

Vent Area and Room Volume for Explosion Rooms with Initially Covered Vent Areas

The effect of room volume and venting of gas (i.e. mass flow) from the explosion room on the gas pressure history in the explosion room is calculated with the factor $K_d(t)$ in Equation 6 at each time step. The room volume and vent area are constant for rooms with only uncovered vent areas. However, most explosion rooms of interest to the DDESB have covered vent areas, consisting of lightweight wall and/or roof panels that are intended to fail quickly (i.e. failure of their attachment to the supporting beams) in an explosion and provide large vent areas as they are blown away from the building. The vent area $A_v(t)$ for an explosion room with initially covered vent areas is calculated with Equation 8. The perimeter vent area in Equation 8 is equal to the displacement of the vent cover, minus any recessed depth of the failed vent cover relative to surrounding wall thickness or wall height that delays venting, multiplied by the perimeter around the vent cover where venting can occur. This is illustrated in Figure 5, where venting is delayed until the vent cover can occur along three sides of the vent cover (or vent panel), and cannot occur along the ground surface. The displacement of the vent covers in Equation 8 is calculated with Equation 9. Equation 9 assumes the vent cover accelerates as a rigid body after it fails based on the net pressure acting on its surface area. It also includes the initial velocity from the shock impulse applied over the surface of the vent cover. This shock impulse can be reduced by the impulse absorbed by the vent cover prior to failure (i.e. impulse that would cause the vent cover to just barely fail with zero velocity). However, vent walls and vent covers are typically attached with low strength screws to facilitate very quick failure of the walls, which minimizes the absorbed energy so that it is neglected. This was the case for all the available test data.

$$A_v(t) = A_{uc} + \sum_0^{j_{max}} A_{pj}(t)$$

$$A_{pj}(t) = (d_j(t) - t_{wj})P_{dj} \quad \text{where } 0 \leq A_{pj}(t) \leq A_{cj}$$

Equation 8

where:

- $A_v(t)$ = total vent opening area at time t
- A_{uc} = total uncovered vent area
- $A_{pj}(t)$ = perimeter vent area around j^{th} failed vent cover at time t
- A_{cj} = surface area of j^{th} failed vent cover
- t_{wj} = recessed depth of j^{th} failed vent cover before venting can occur
- $d_j(t)$ = displacement of j^{th} failed vent cover (see Equation 9)
- P_{dj} = perimeter distance around j^{th} failed vent cover available for venting
- j_{max} = total number of covered vent openings

$$d_j(t) = v_{oj} + \int_{t_f}^{t_g} \left(\frac{P_g(t) - K_{gr}m_jg - D_f}{m_j} \right) dt$$

$$v_{oj} = \frac{i_{rj} - i_{fj}}{m_j}$$

Equation 9

where:

- $d_j(t)$ = displacement of j^{th} failed vent cover at time t
- t_f = failure time of j^{th} failed vent cover
= 0 (default)
- t_g = duration of gas pressure in room
- m_j = mass per unit area of j^{th} failed vent cover
- $P_g(t)$ = net pressure acting on vent cover at time t (e.g. gas overpressure in explosion room)
- g = gravity constant
- i_{rj} = average applied shock impulse on j^{th} failed vent cover including internal shock reflections
- i_{fj} = impulse absorbed by strain energy of j^{th} failed vent cover prior to failure
= 0 (default value since it is assumed vent covers are designed to absorb minimal strain energy)
- K_{gr} = gravity load factor
= 1 if vent cover is on roof of building
= 0 if vent cover is on wall of building
- D_f = pressure caused by drag force (typically negligible)

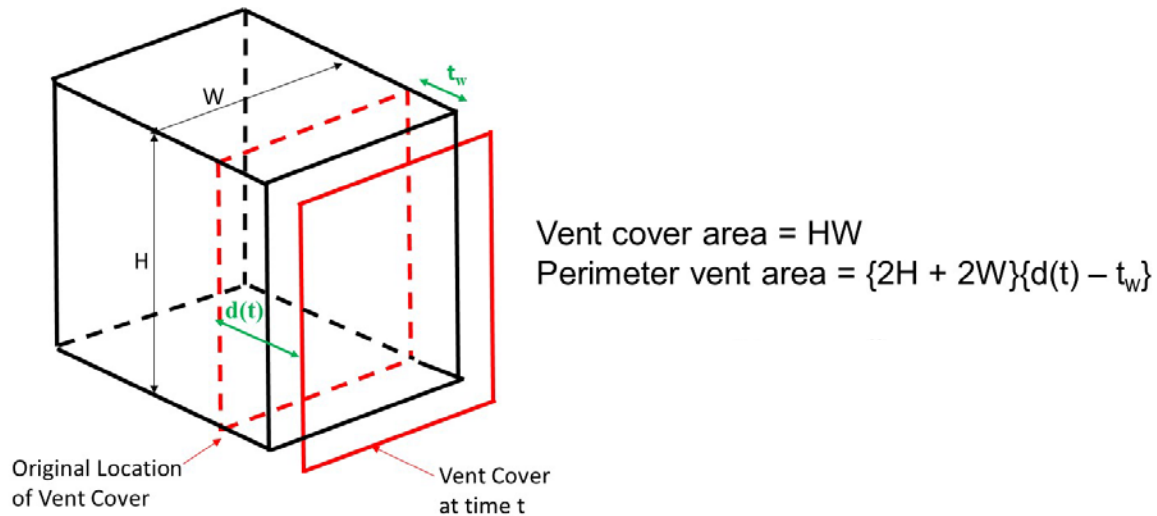
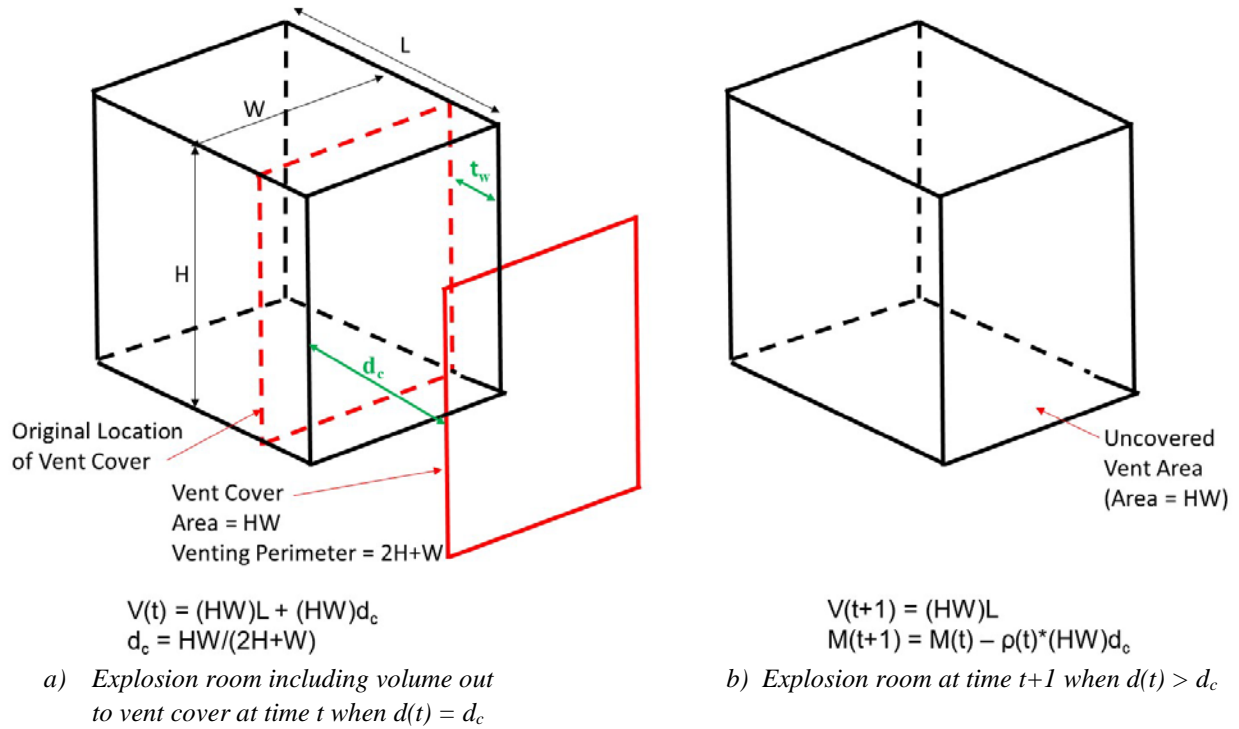


Figure 5. Perimeter Venting due to Vent Cover Displacement

The movement of the vent panels also increases the effective room volume if the thickness or height of walls surrounding the vent cover provides containment (i.e. does not allow venting) over a displacement equal to t_w in Figure 5 during initial movement of the vent cover. However, as the vent panel displaces outward past t_w , the pressurized gas in the room volume must expand to fill up the space created by this outward movement. This implies the pressurized volume continues to increase as the vent cover moves out from the explosion room. However, when the vent cover moves far enough away from the original room volume, the vent cover will not affect the venting process (i.e. there will no longer be perimeter venting) and original volume of the room will vent through the opening (now fully uncovered) in the room. This process is simplistically modeled as follows. The volume of a room with a covered opening includes all the volume contained by a vent cover as it displaces out, away from the explosion room, until the cover displaces to a critical distance, d_c . At the distance d_c , the perimeter vent area around the vent cover is equal to the area of the opening that was initially covered. At the time step when the

vent cover displacement is equal to d_c , the type of venting switches from perimeter venting around the vent cover to venting through the now uncovered opening that was originally covered. This is illustrated in Figure 6. During this time step when the type of venting changes, the room volume reduces to the original room volume plus any volume due to the recessed depth of the vent cover. The mass of gas in the room also reduces during this time step such that the density of the gas does not change. Therefore, the explosion room loses both volume and mass, such that it maintains the same density of gas (and therefore same gas pressure) during this conversion from perimeter venting to venting through the uncovered opening. During the remainder of the gas pressure history, the room volume does not change (unless there are other initially covered openings) and the mass of gas in the reduced volume continues to flow out of the uncovered vent area equal to WH in Figure 6. The room volume at each time step during this process is calculated with Equation 10.



Note: $V(t)$ = room volume at time t , $M(t)$ = mass of gas in room at time t , $\rho(t)$ = density of gas in room at time t
 $t+1$ is the next time step

Figure 6. Mass and Volume in Explosion Room Before and After Critical Displacement of Vent Cover

$$V(t) = V_o + \sum_0^{jmax} \Delta V_j(t)$$

$$\Delta V_j(t) = d_j(t)A_{c_j} \quad \text{for } d(t) \leq d_{c_j} \quad \text{where } d_{c_j} = t_{w_j} + \frac{A_{c_j}}{P_{d_j}}$$

$$\Delta V_j(t) = t_{w_j}A_{c_j} \quad \text{for } d(t) > d_{c_j}$$

Note: Mass of gas in room is adjusted to cause no change in density during first time step when $d(t) > d_c$

Equation 10

where:

$V(t)$ = effective room volume with gas pressure at time t
 $\Delta V_j(t)$ = additional volume of air between vent cover and original position of vent cover at time t
 V_o = initial room volume
 $d_j(t)$ = displacement of j^{th} failed vent cover at time t from Equation 9
 A_{c_j} = surface area of j^{th} failed vent cover
 P_{d_j} = perimeter distance around j^{th} failed vent cover available for venting
 A_{c_j} = surface area of j^{th} failed vent cover
 t_{w_j} = recessed depth of j^{th} failed vent cover before venting can occur
 d_{c_j} = critical displacement of vent cover when venting switches from perimeter venting to venting through uncovered opening with area equal to vent cover area
 j_{max} = total number of covered vent openings

Explosion Room Mass Loss Due to Venting

The effect of mass loss due to gas venting from the explosion room on the gas pressure history is calculated with the factor $K_d(t)$ in Equation 6 at each time step. The initial mass in the explosion room is the mass of air in the room plus the mass of the explosive. The mass changes at each time step based on venting (i.e. mass outflow) from the explosion room through the vent area $A_v(t)$ calculated with Equation 8. The mass loss at each time step is calculated with Equation 11, which is based on isentropic mass flow through a nozzle. The mass change is a function of the flow area (i.e. vent opening area), the gas pressure in the explosion room, the density of venting gas, and the empirical discharge coefficient. The equation for choked flow in Equation 11 is used whenever the absolute gas pressure exceeds approximately 2 bar. The ratio of specific heats for the venting gas from the explosion room is assumed constant at 1.4 representing air at standard temperature and pressure.

$$M(t) = \frac{dM(t)}{dt} \Delta t + M(t-1)$$

$$\text{If } \left(\frac{P(t)}{P_o(t)} \right) \leq 0.53, \frac{dM}{dt}(t) = S_d(t) A_v(t) \sqrt{\gamma \left(\frac{2}{\gamma+1} \right) \rho(t) P(t)} \text{ (this is choked flow)}$$

$$\text{Else } \frac{dM}{dt}(t) = S_d(t) A_v(t) \sqrt{2 \rho(t) P(t) \left(\frac{\gamma}{\gamma-1} \right) \left(\left(\frac{P(t)}{P_o(t)} \right)^{\frac{2}{\gamma}} - \left(\frac{P(t)}{P_o(t)} \right)^{\frac{\gamma+1}{\gamma}} \right)}$$

Equation 11

where:

$M(t)$ = mass of gas in explosion room at time t
 Δt = time step
 $dM(t)$ = mass flow through a vent opening during Δt time t
 dM/dt = mass flow rate through all vent opening at time t
 $S_d(t)$ = discharge coefficient (see Equation 12)
 $P(t)$ = absolute gas pressure in room at time t
 $P_o(t)$ = atmospheric pressure for venting to the atmosphere at all time steps = 14.7 psi
 $\rho(t)$ = density of gas in room at time t
 $A_v(t)$ = flow area through vent openings at time t (see Equation 8)
 γ = ratio of specific heats (1.4 for air)

The value of the discharge coefficient S_d in Equation 11 was initially assumed equal to a constant value of 0.62 based on information shown in Figure 7 (Blevins, 2003). This assumes that there is essentially no “nozzle” to streamline the mass flow through vent areas, resulting in the minimum value of measured values of S_d equal to 0.61. However, analyses using this improved methodology in near final form tended to overcalculate the impulse a significant number of tests with uncovered vent area, where the methodology was matching the measured maximum gas pressure well. Higher values of S_d allow faster blowdown, which cause a lower calculated impulse. Therefore, Equation 12 was developed empirically using curve-fitting and trial and error to minimize the difference between

the calculated gas pressure impulse and measured values from tests with initially covered and uncovered vent areas in analyses. In these analyses, the calculated peak gas pressure was forced to be exactly equal the measured peak gas pressure in each test to make sure any differences between calculated and measured maximum gas pressure would not affect the empirical equations developed for the discharge coefficient. The resulting curve-fit equations in Equation 12 indicate that the discharge coefficient for uncovered vent areas is a function of the loading density at higher loading densities and a function of the scaled vent area at lower loading densities, varying from 0.72 to 1.0. The discharge coefficient is equal to a constant value of 0.61 for a covered vent area while the vent cover affects the vent area. After the vent cover has moved far enough from the room so that the initially covered area acts as an uncovered vent area, the discharge coefficient is calculated as for an uncovered vent area. The discharge coefficient and mass flow are calculated separately for each opening in the explosion room are at each time step.

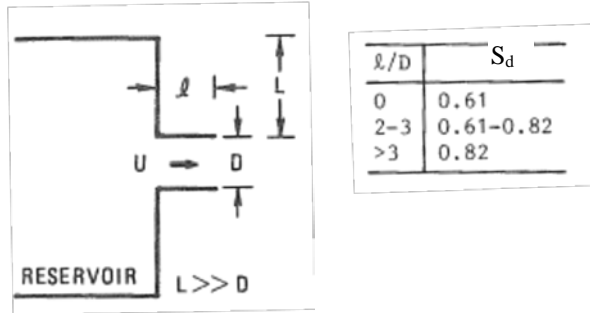


Figure 7. Discharge Coefficient, S_d (from Blevins, 2003)

For initially covered vent areas while $d(t) \leq d_c$:

$$S_d(t) = 0.61$$

For uncovered vent areas:

$$\text{if } \left(\frac{W_{Eg}}{V(t)} \right) < 0.02 \frac{lb}{ft^3} \quad S_d(t) = 0.8 \left(\frac{A_{uc}}{V(t)^{\frac{2}{3}}} \right) + 0.61 \leq 1.0$$

$$\text{Else} \quad S_d(t) = 0.76 \frac{W_{Eg}}{V(t)} + 0.74 \leq 1.0$$

Equation 12

where:

$S_d(t)$ = discharge coefficient for Equation 11

A_{uc} = uncovered vent area

$V(t)$ = confined volume during time step calculated using Equation 10

W_{Eg} = equivalent TNT charge weight to calculate peak gas pressure per UFC 3-340-02

$d(t)$ = displacement of vent cover at time t calculated with Equation 9

d_c = critical displacement of vent cover when venting type changes to uncovered venting
(see Figure 6)

The discharge coefficient, S_d , in Equation 11 is accounting for numerous physical complexities that are not accounted for in the simplified mass flow equation. This includes vortices at the edges of the flow area, curved flow lines from the pressurized volume through the flow area, and possible reduced gas pressure in the volume between a vent panel and the explosion room (i.e. the volume within d_c in Figure 6) that is forcing mass flow through the perimeter vent area. This latter factor may be the reason that the empirical value of the discharge coefficient is lower for covered openings than uncovered openings in Equation 12. Also, all pressure drop during venting is simplistically attributed to mass flow in the enhanced method, whereas some pressure drop is caused by a lowered temperature due the venting of hot gases and other phenomena. All factors affecting the reduction in the gas pressure, other than mass flow, are implicitly included in the discharge coefficient since it is the only empirical part of the methodology for the blowdown phase of the calculated gas pressure history. The curve-fit equations that are

the basis for Equation 12 caused correlation coefficients (i.e. R^2 values) between calculated gas pressure impulse and measured impulse from the test data that were not very high (i.e. in the range of 0.6 to 0.7), so future testing or analysis that can provide an improved understanding of the venting process would be helpful for improving the gas pressure history prediction methodology.

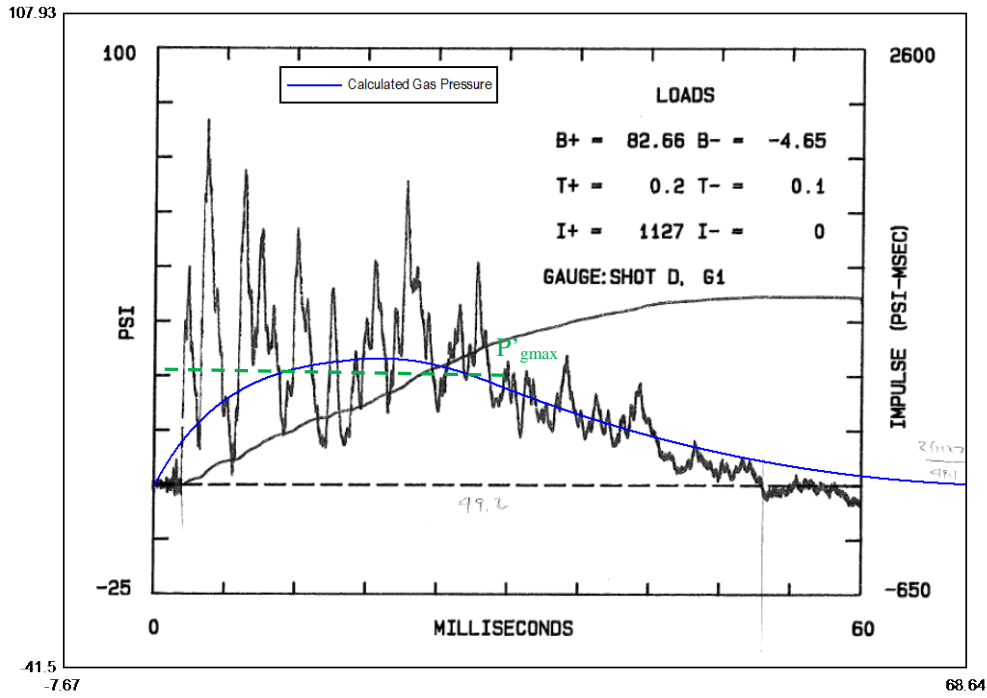
Comparisons of Calculated and Measured Gas Pressures

Figure 8 shows typical comparisons between gas pressure histories calculated with the improved gas pressure prediction method and measured gas pressure histories. The gages from gas pressure tests typically measured a significant amount of unintended shock pressure in addition to the gas pressure, as evidenced by the high frequency content of some of the measured pressure history in Figure 8. The calculated gas pressure generally matches the low frequency portion of the measured gas pressure histories well for all the available measured gas pressure histories, as shown in Figure 8. The maximum measured gas pressure was subjectively determined for each gage of each test in the database with a measured gas pressure history, equal to P'_{gmax} , as illustrated in Figure 8. The values of P'_{gmax} for tests with multiple gages were averaged to get the final value of P'_{gmax} for the test with multiple gas pressure gages. The percentage error between the calculated maximum gas pressure and P'_{gmax} was calculated and plotted for each applicable test in the gas pressure database in Figure 9.

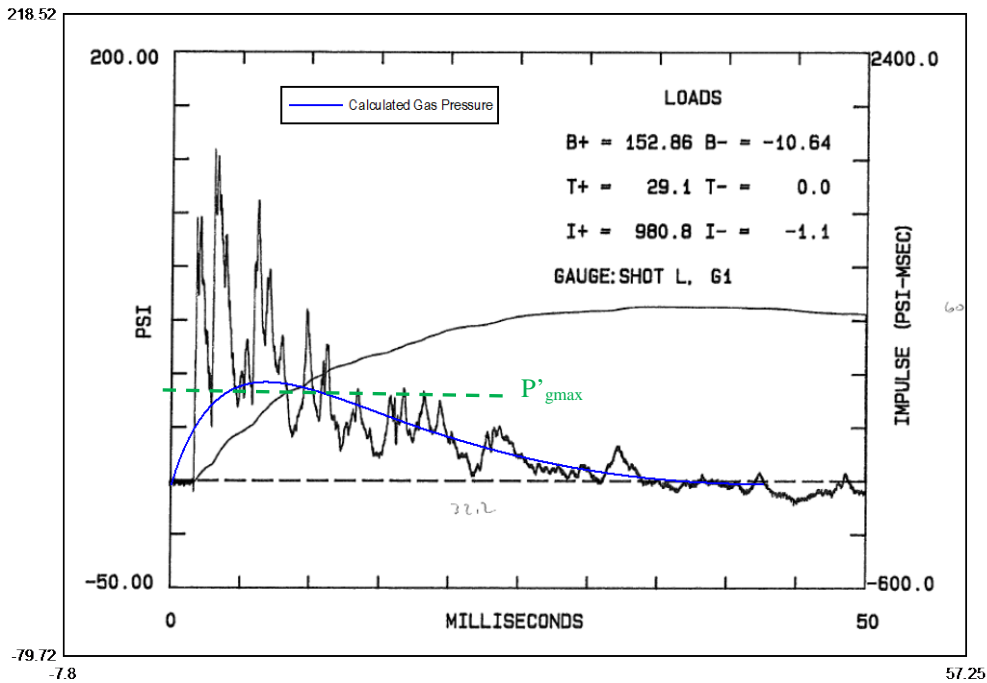
Figure 9 should be interpreted understanding the variability inherent in the measured maximum gas pressures, which is caused by the engineering judgement required to determine the peak gas pressure from the measured pressure history due primarily to the unintended shock pressure that is measured by the gas pressure gages. A study of the variability of the peak gas pressures reported at various gages in the same test for 4 test series with multiple gas pressure gages per test showed a coefficient of variation (COV) between 5% and 20% (Oswald, 2017). This is an average COV of 12%. A COV of 12% for a standard, or normal probability distribution implies that 68% of the measured peak gas pressures for each test were within 12% of the average measured peak pressure for the test and 95% of the of the measured peak gas pressures were within 24% of the average value. This is due to scatter in the measured gas pressures because theoretically all the pressure gages in a given test should measure the same peak gas pressure. Based on this observation, it is reasonable to expect that an “accurate” prediction method would also calculate maximum gas pressures that have at least this same variability compared to the average measured maximum gas pressures. The legends in Figure 9 indicate that the improved method is accurate compared to the average measured maximum gas pressure when viewed from this perspective. Table 1 shows statistics for the percent error values for each test in Figure 9. It shows that, on the average, the maximum gas pressure is calculated very accurately by the improved method compared to the test data, and that the coefficient of variation of the error is within the range of 12% that can be attributed to variability in measured peak gas pressures. Table 1 also shows that the improved method is much better at calculating the measured maximum gas pressure than the FRANG and BlastX programs that are currently used. These statistics are based on percent error information for the calculated peak gas pressure reported by Oswald (2017). An apparent large conservatism in the calculated peak gas pressures with the FRANG code based on accident investigations has also been reported and discussed by Bogosian and Zehrt (1998).

Comparisons of Calculated and Measured Gas Pressure Impulses

The error between the gas impulse calculated with improved method and the average measured impulse for each test in the gas pressure database with venting was also calculated. Table 2 shows statistics for the percent error in the calculated impulses for these tests with uncovered vent areas and initially covered vent areas. Figure 10 show plots of the error in the calculated impulse vs. scaled vent area for tests with uncovered and covered vent areas. The average error in the calculated impulse and the standard deviation of the error are both somewhat higher than the corresponding values for the error in the calculated maximum gas pressure.



a) Comparison for test with covered vent area



b) Comparison for test with uncovered vent area

Figure 8. Calculated and Measured Gas Pressure Histories

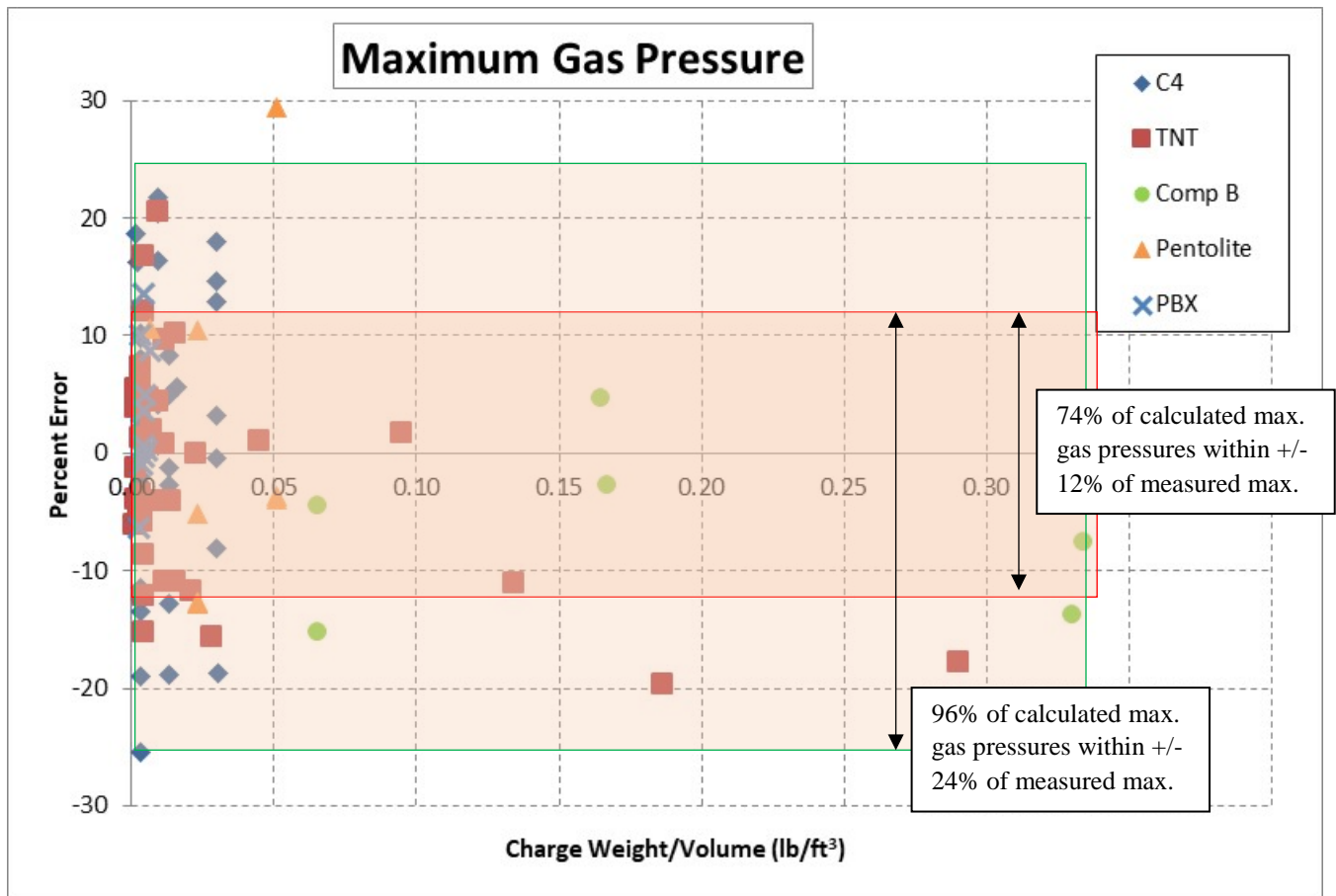


Figure 9. Error in Calculated Maximum Gas Pressures with Enhanced Method

Table 1. Percent Error in Maximum Gas Pressure Calculated with Improved Method

Methodology	Case	Average Error (%) ¹	Standard Deviation of Error (%)	Coefficient of Variation (%)
Improved Methodology	Fully confined tests ²	1.7	11.1	9
	Tests with uncovered vent areas	0.6	11.5	11
	Tests with initially covered vent areas	2.7	12.7	10
FRANG ³	All	16	30	192
BlastX ³	All	30	38	132
Gas Pressure Tests	Reported maximum gas pressure in tests with multiple gages ⁴			12

Note 1: Percent error is equal to the ratio of the calculated maximum gas pressure minus the measured maximum gas pressure divided by the measured gas pressure expressed as a percentage.

Note 2: Tests with a scaled vent area ($A/V^{2/3}$) less than 0.015.

Note 3: Based on information in Oswald (2017).

Note 4: The COV of peak gas pressures measured at various gages in the same test varied from 5% to 20% in 4 test series where detailed gas pressure measurements are reported (Oswald, 2017). This is an average value of 12%.

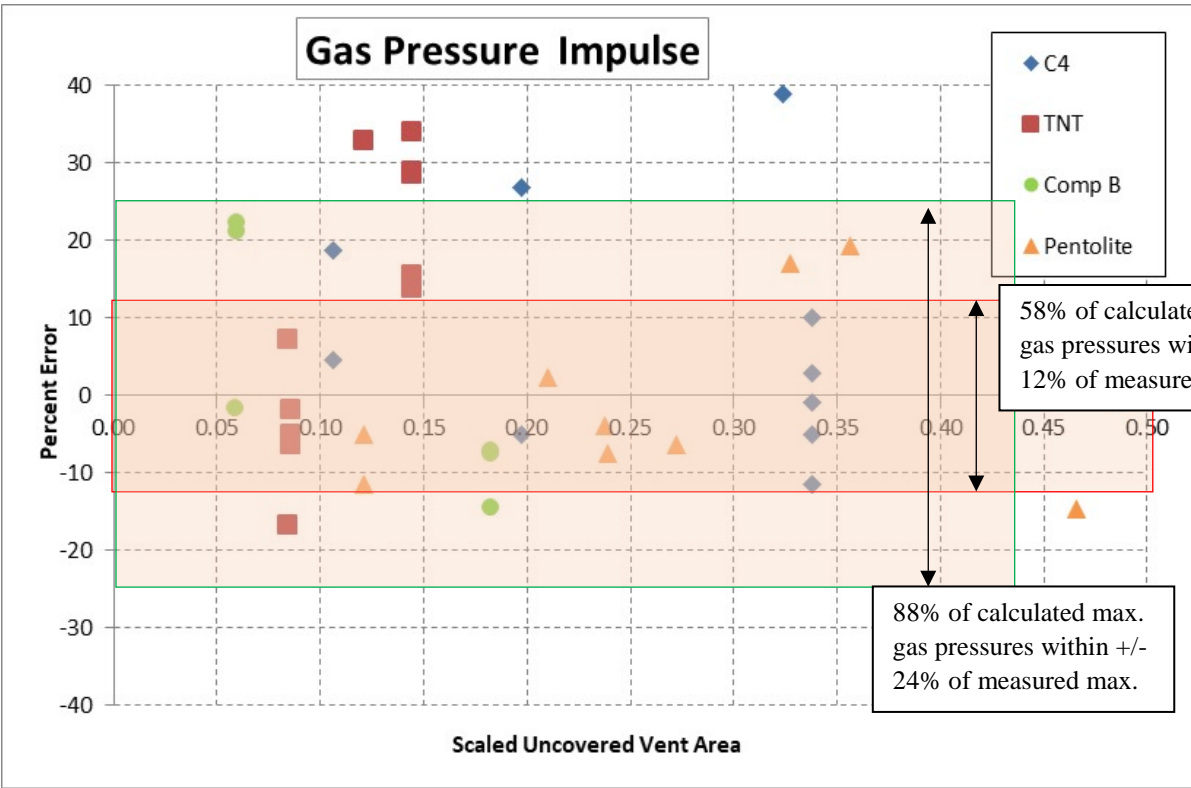
Table 2. Percent Error in Gas Impulse Calculated with Enhanced Method

Methodology	Case	Average Error (%) ¹	Standard Deviation of Error (%)	Coefficient of Variation (%)
Improved Methodology	Tests with uncovered vent areas	3.4	14.5	11
	Tests with initially covered vent areas	-3.8	14.5	10
FRANG ²	All	29	42	146
BlastX ²	All	27	45	170
Gas Pressure Tests	Reported maximum gas pressure in tests with multiple gages ³			12
<p>Note 1: Percent error equal to the ratio of the calculated maximum gas pressure minus the measured maximum gas pressure divided by the measured gas pressure expressed as a percentage.</p> <p>Note 2: Based on information in Oswald (2017).</p> <p>Note 3: The COV of peak gas pressure impulses measured at various gages in the same test varied from 5% to 20% in 4 test series where detailed gas pressure measurements are reported (Oswald, 2017). This is an average value of 12%.</p>				

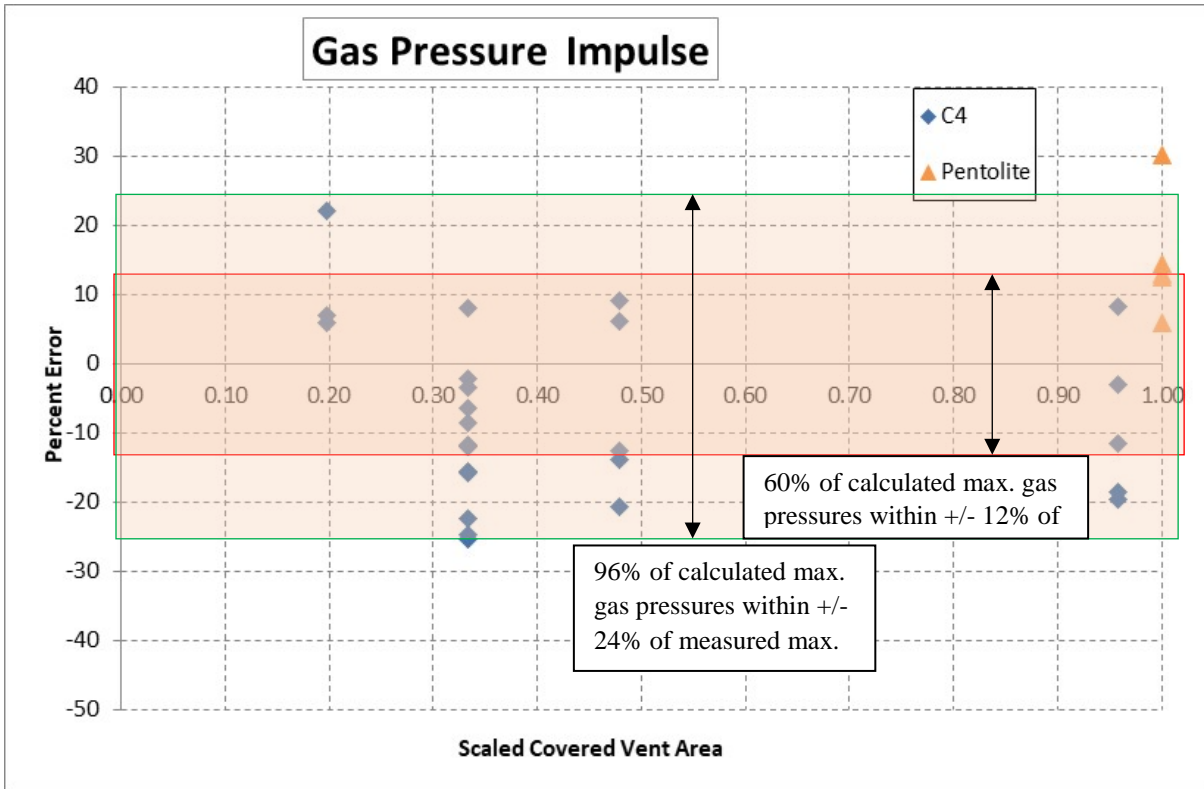
Figure 10 shows that most of the calculated impulses were within +/- 12% of the measured impulses (i.e. 58% of the tests) and a much larger percentage were within +/- 24% (i.e. 88% of the tests). However, these percentages are less than the desired values of 68% and 95% that would indicate an “accurate” prediction method that has the same variability compared to the average measured impulse as the measured impulses. Therefore, these percentages and the information in Table 2 (i.e. the average error of 3% to 4%) both indicate there is somewhat more error in the calculated impulse than can be explained by only the variability in the measured impulses, although not an excessive amount. Both plots in Figure 10 indicate no observable trend in the accuracy of the calculated impulses based on scaled vent area or charge type of the tests. A plot of the error in calculated impulse vs. loading density also shows no trend in the accuracy of calculated impulse based on loading density of the tests. Therefore, there is no apparent systematic error in the calculated impulses compared the measured impulses. Also, the coefficient of variations in Table 2 is consistent with the variability in the measured impulses. In summary, the error shown in Table 2 and Figure 10 indicates the impulse is calculated less accurately compared to the test data with the enhanced method than the peak gas pressure, but it is within the range of accuracy that is typically considered acceptable for a fast-running methodology. Table 2 also shows that the improved method is much better at calculating the measured gas impulse than the FRANG and BlastX programs that are currently used. These statistics are based on percent error information for the calculated peak gas pressure reported by Oswald (2017).

Summary of Comparison of Calculated to Measured Gas Pressures

The maximum gas pressure and impulse calculated with the current improved gas pressure prediction method are accurate, on the average, compared to the measured gas pressure histories (i.e. within 5%) in a large gas pressure database gathered for the DDESB. Also, the coefficient of variation of the errors is within the range that can be explained by the variation within the measured gas pressure parameters for each test. Finally, Figure 8 shows generally representative comparisons between calculated and measured gas pressure histories indicating that the calculated gas pressure histories have a similar form as the measured gas pressure histories. The shapes of the calculated gas pressure histories in Figure 8 match the shape of the measured gas pressure histories much better than gas pressure histories calculated with the existing methods that assume a very sharp rise (nearly zero rise time) to the peak gas pressure up to a pressure based on full confinement. This is due to the fact the improved method calculates a gas pressure rise time, it accounts for the effects of volume change, mass loss, and energy losses from venting during the rise time on the maximum gas pressure (i.e. reducing the maximum gas pressure), and it calculates the blowdown phase of the gas pressure history more accurately by using a theoretically based approach with an empirical calculated discharge coefficient for mass flow through vent areas.



a) Tests with Uncovered Vent Areas



b) Tests with Initially Covered Vent Areas

Figure 10. Error in Calculated Gas Impulses with Enhanced Method

References

1. Bessette, Greg and Emmanuelli, Gustavo, "Gas Phase Calculations – BlastX," Prepared for Air Force Research Laboratory, AFRL, U.S. Army Engineer Research and Development Center (ERDC) BlastX Methodology Report 2014-001a, October 2014.
2. Blevins, Robert D., *Applied Fluid Dynamics Handbook*, Krieger Publishing Co., Malabar, FL, 2003.
3. Bogosian, David D. and Zehrt, William H., "Assessment of Analytical Methods Used to Predict the Structural Response of 12-inch Concrete Substantial Dividing Walls to Blast Loading," Proceedings of the Twenty-Eighth DoD Explosives Safety Seminar, Orlando, FL, August 1998.
4. ERDC, "BlastX Computer Program - Blast and Thermal Environment for Internal or External Explosions", Version 6.4.2.2, U.S. Army Engineer Research and Development Center (ERDC).
5. NAVFAC ESC, "Confined Blast Code (CONBlast) V1.1.18.140," Distributed by NAVFAC ESC, 2015.
6. Hager, Kevin, Needham, Charles and Doolittle, Craig, "Algorithm for Calculating Gas-Pressure Rise-Time for Confined Explosions," Proceedings of the Thirty-Second DoD Explosives Safety Seminar, Philadelphia, Pennsylvania, August 2006.
7. Keenan, W.A. and P.C. Wager, "Mitigation of Confined Explosion Effects by Placing Water in Proximity of Explosives," Proceedings of the 25th DoD Explosives Safety Seminar, Anaheim, CA, August, 1992.
8. Kuhl, A. L., Forbes, J., Chandler, J., Oppenheim A. K., Spektor, R., Ferguson, R. E., "Confined Combustion of TNT Explosion Products in Air," 8th International Colloquium on Dust Explosions Schaumburg, IL, September, 1998.
9. Oswald, C. "Comparison of Measured and Calculated Gas Pressure Histories," Proceedings from the 17th International Symposium on the Interaction of the Effects of Munitions with Structures, Bad Neuenahr, Germany, October, 2017.
10. Proctor, James F., "INTERNAL Blast Damage Mechanisms Computer Program, "Naval Ordnance Laboratory Report No. AD-759 002, Prepared for Air Force Flight Dynamics Laboratory, August 1972.
11. Tancreto, J. E. and Helseth, E. S., "Effect of Frangible Panels on Internal Gas Pressures," Minutes of the 21st DDESB Explosives Safety Seminar, 1984.
12. Wager, P. and Connett, J., "FRANG User's Manual," Naval Civil Engineering Laboratory, Port Hueneme, CA, May 1989.
13. UFC 3-340-02, Change 2, "Structures to Resist the Effects of Accidental Explosions," Dept. of Defense, Washington, DC, USA, 2014.
14. Weibull, H. R. W., "Pressures Recorded in Partially Closed Chambers at Explosion of TNT Charges (U)", *Annals of the New York Academy of Sciences*, Vol. 152, Art. 1, 1968.